Tectonic history and occurrence of 2.4 Ga mafic dyke swarms adjacent to Godavari Basin, Karimnagar, India

J. Mallikharjuna Rao[1,*], G. V. S. Poornachandra Rao[1], M. Widdowson[2], T. Yellappa[1] and S. P. Kelley[2]

[1]National Geophysical Research Institute, Hyderabad 500 007, India
[2]Department of Earth Sciences, The Open University, Milton Keynes, UK

Proterozoic dyke swarms are exposed partly in granulitic terrain and partly in gneissic terrain and extend in a NE–SW direction near the Godavari Basin, Karimnagar area, Central India. The Karimnagar dyke swarm petrographically exhibits two groups such as fresh plagioclase and pyroxene phenocrystic dolerite dykes and altered non-phenocrystic gabbros. Dolerites show ophitic to subophitic textures and gabbros are non-porphyritic and more altered. Geochemical data suggests that these dykes are tholeiitic in nature, range from basalt to basaltic andesite in composition. The rare earth element patterns show enrichment of light rare earth elements (25–60 times) and heavy rare earth elements show flat patterns (4–10 times) supporting the presence of two varieties within the dyke swarm. A laser probe $^{40}Ar/^{39}Ar$ study and Ar isotopic analyses suggest two magmatic emplacement ages at 2400 Ma and 2200 Ma which are present within the dyke swarm. Palaeomagnetic results reveal a characteristics remnant magnetization vector of $D_m = 52.5$, $I_m = -24.5$ ($K = 21.81$, $\alpha_{95} = 8.65°$, $N = 12$) and supports the presence of two phases of dyke activity in the region.

Keywords: Geochemistry, geochronology, Karimnagar, mafic dykes, palaeomagnetism.

MAFIC dyke swarms are one of the remnants of mafic magmatism related to the breakup of 2.5 Ga supercontinent[1], which are so abundant and extensive that they reasonably constitute large igneous provinces[2–4]. The huge number of mafic dykes and associated igneous rocks worldwide intruded during 2.45–2.1 Ga probably resulted from episodic, semi-continuous attempts at subsequent continental breakup. The mafic dykes are considered as manifestation of extensional tectonics and intraplate magmatism. The numerous dykes and dyke swarms in the south Indian peninsular shield indicate periodic crustal dilation during early-late Proterozoic period[5,6]. Global periodicity of dyke emplacements at 2400, 1800, 1000 and 600 Ma is well preserved in the Indian shield[5,7,8]. The Karimnagar area, north of the Cuddapah Basin located in the central part of the Indian peninsula, consists of a variety of rock types of different ages and lithologies occurring along flanks of the Pranhita–Godavari rift basin shown in Figure 1. The area lies between the Archaean low-grade terrane of the eastern block of Dharwar craton (EDC) to the southwest and the Pakhal–Sullavai (middle-late Proterozoic) and Gondwana (Palaeozoic–Mesozoic) formations of the Pranhita–Godavari Graben to the northeast. An overview of the geochronological and tectonic aspects of the Karimnagar Granulite Belt (KGB), Bhopalapatnam Granulite Belt (BGB) and surrounding geological domains was given by Santosh[9]. The Karimnagar dyke swarm extends in a NE–SW direction adjacent to the Mesoproterozoic Pakhal Basin and Godavari Basin for about 125 km with many of the dyke segments showing local variation from NE–SW, ENE–SWS, E–W and rarely N–S directions[10]. The Archaean basement of Karimnagar area consists of a variety of rock types such as gneisses, metasediments, granites, acid and basic dykes

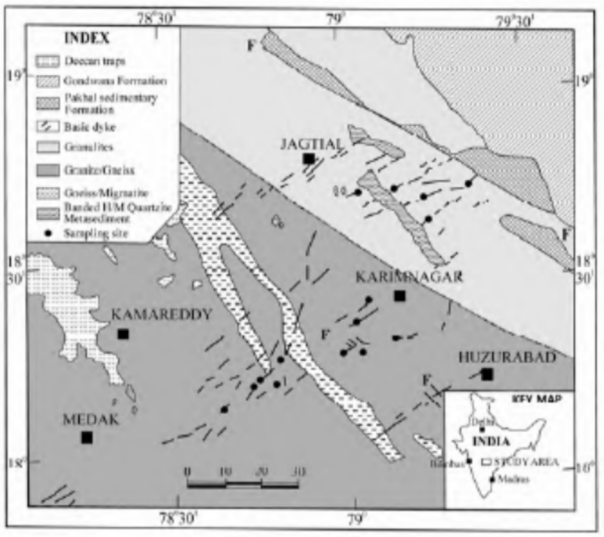

Figure 1. Geological map of Karimnagar area showing dykes and sampling sites for palaeomagnetic and other studies.

*For correspondence. (e-mail: mallikharjun_ngri@yahoo.co.in)

and newly discovered granulite terrain[11,12]. In the northeastern part of the study area, Mesoproterozoic Pakhal and Sullavai formations of the Purana Group consisting of orthoquartzites, banded magnetite quartzite, sandstone, shale and limestone are exposed. The dyke/dyke swarm is exposed partly in granulitic region and partly in basement gneissic terrain. The two types of dykes present in the area namely porphyritic and gabbroic dykes do not show marked differences in field outcrops and are mostly oriented in NE–SW direction.

Petrography and geochemistry

The Karimnagar dyke swarm is represented by two varieties of rocks namely fine-grained, fresh, porphyritic dolerites and altered non-porphyritic gabbros. Dolerites generally show ophitic to subophitic textures. In porphyritic types, orthopyroxene of hypersthene composition is rarely present and augite and plagioclases are the phenocrysts (10–15 vol%). The essential minerals are plagioclase (35–42 vol%, oligoclase to labradorite) with oscillatory compositional zoning, clinopyroxene (32–35 vol%) of augite composition and with or without hypersthene and secondary minerals (5 vol%) like hornblende, calcite and chlorite are seen as partly developed rims over pyroxenes. The opaque minerals are ilmenite and magnetite (4–5 vol%). Ilmenite is seen altered to sphene. Granophyric intergrowths are present as interstitial grains in these rocks. Dolerites exposed in the granulite terrain show differences in terms of strong clouding, bent twin lamellae in plagioclase and undulatory extinction in pyroxenes. Absence of such features in dolerites and gabbros of non-granulitic terrain is clear. The granulite metamorphism in the region and upliftment of deeper parts to the present level reflects in clouding, strong undulatory extinction, bent twin lamellae in minerals of deformation. They also show relict igneous textures. The gabbroic samples are non-porphyritic and show plagioclase (40–45 vol%, labradorite), titaniferous augite (35–40 vol%) and altered minerals (10–12 vol%) along the grain boundaries and conspicuous absence of granophyric intergrowths. The opaque minerals are magnetite (2–3 vol%) and ilmenite (1–2 vol%) that occur as small discrete grains or needles distributed throughout the rock.

All the dykes are tholeiite in composition and range from basalt to basaltic andesite in composition (Figure 2) and are either quartz normative or olivine normative in nature. Total alkalies–iron–magnesium ternary plot indicates that the quartz normative types are less enriched in iron than the olivine normative types and show a calc-alkaline trend of differentiation. Geochemical data (Table 1) of one sample (KR65) shows higher MgO (11.98%), FeO (11.06%) and lower Al_2O_3 (11.67%), SiO_2 (49.7%) and CaO (5%) compared to the other group of samples; we infer it may be due to rare presence of hypersthene phenocrysts in the rock and more mafic enriched sample in the dyke swarm. Rare earth elements (REE) are moderately enriched (ΣREE = 22–63.5 ppm) and light REE show enriched patterns (La_N/Sm_N = 3.5–10.1) and heavy REE show flat trends (Gd_N/Yb_N = 0.7–1.2) as evident from Figure 3. Most of the samples show negative Eu anomaly (Eu/Eu* = 0.67–0.98) which may be due to early removal of plagioclase from the melt. REE patterns clearly indicate two groups and correspond to olivine normative and quartz normative types. Primitive mantle normalized multielemental spidergram is of olivine normative type showing distinct negative Nb, Sr, P and Ta troughs suggesting that they are contaminated by crustal materials whereas quartz normative types show relatively flat trends suggesting that they have less interaction with crustal materials (Figure 4). Tectonic discriminant diagrams show that these dykes exhibit mid-oceanic ridge basalt characteristics and progressive enrichment of iron during crystallization[7].

Radiometric ages

$^{40}Ar/^{39}Ar$ ages of dolerite dykes were estimated by laser ablation technique at the Open University, Milton Keynes, UK. The GA 1550 biotite standard with an age of 98.79 ± 0.96 Ma was used to monitor the fast-neutron flux and the calculated J value is 0.01047 ± 0.000055. The samples were irradiated at the McMaster Reactor in Canada. Noble gases were equilibrated into a high sensitivity MAP 215-50 noble gas mass spectrometer and extracted argon ^{35}Ar to ^{41}Ar isotopes were measured. Representative 10 min extraction system blank measurements obtained during the experiments were $^{40}Ar = 9 \times 10^{-12}$; $^{39}Ar = 2 \times 10^{-14}$; $^{38}Ar = 3 \times 10^{-14}$; $^{37}Ar = 7 \times 10^{-13}$

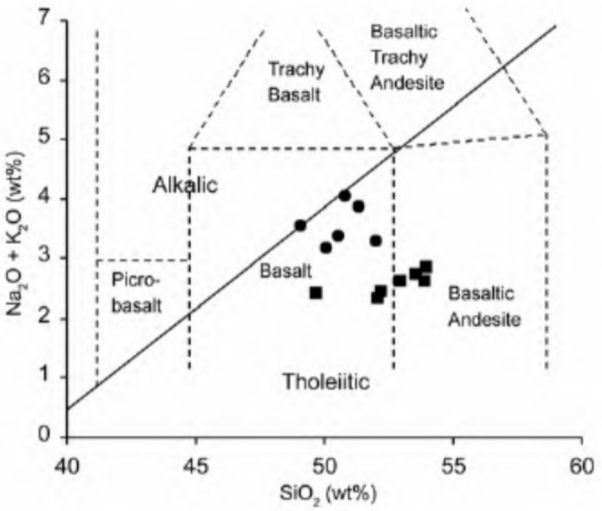

Figure 2. Total alkalies and silica diagram showing classification of different rock types. Demarcation fields are from refs 23 and 24. Solid circle – olivine normative dykes and solid square – quartz normative dykes.

Table 1. Chemical data of Karimnagar dykes

	KR51	KR52	KR53	KR54	KR56	KR57	KR60	KR61	KR63	KR65	KR66	KR68	KR69
SiO_2	52.19	52.92	53.93	53.90	52.06	53.50	49.09	50.08	50.55	49.68	51.99	51.33	50.81
TiO_2	0.51	0.52	0.58	0.52	0.41	0.50	0.92	0.92	1.00	1.65	0.53	1.04	1.00
Al_2O_3	13.71	13.28	14.87	14.05	12.61	14.14	13.03	13.30	13.70	11.67	13.67	12.63	12.96
Fe_2O_3	2.28	2.45	2.69	2.42	2.79	1.76	3.53	2.98	3.12	4.30	2.18	3.98	3.62
FeO	7.80	7.96	7.08	6.89	8.20	8.20	10.08	10.48	10.20	11.06	8.36	8.78	10.05
MnO	0.10	0.16	0.08	0.1		0.16	0.18	0.18	0.22	0.14	0.15	0.17	0.17
MgO	8.87	8.64	7.72	7.89	8.64	8.83	8.72	9.73	8.19	11.98	8.98	8.76	6.97
CaO	10.38	10.75	8.23	9.24	10.08	10.46	9.96	10.37	10.05	4.94	10.98	9.32	9.84
Na_2O	2.05	2.00	1.75	1.98	1.87	2.25	2.87	2.62	2.75	2.00	2.87	3.00	3.37
K_2O	0.40	0.62	1.11	0.65	0.47	0.49	0.69	0.55	0.62	0.43	0.43	0.88	0.69
P_2O_5	0.13	0.03	0.01	0.09	0.10	0.04	0.01	0.26	0.14		0.06	0.09	0.05
Total	98.42	99.33	98.05	97.73	97.23	100.33	99.08	101.47	100.54	97.85	100.20	99.98	99.53
Trace elements (ppm)													
Sc	21	18	16	17	28	21	20	20	23	19	22	22	21
V	172	156	139	145	174	179	224	243	262	265	192	264	256
Cr	382	461	332	392	645	391	119	143	56	60	329	129	129
Co	67	66	67	62	81	66	83	82	86	96	96	90	83
Ni	200	130	149	162	209	152	132	131	108	77	143	131	125
Cu	80	88	86	78	99	98	190	184	188	1	115	201	191
Zn	79	76	82	81	82	80	119	116	131	136	80	117	110
Ga	5	2	8	6	5	4	9	8	10	6	4	9	10
Rb	18	16	25	13	6	8	9	6	8	9	5	14	9
Sr	61	69	56	56	51	60	81	71	65	7	56	92	84
Y	9	7	11	10	9	10	15	14	16	20	7	16	15
Zr	38	24	49	39	28	21	41	36	34	45	21	43	40
Nb	29	39	42	32	40	42	40	1	1	3	1	1	2
Cs													
Ba	118	162	221	181	114	121	169	169	159	25	96	168	151
Hf	1.38	0.32	2.18	1.40	0.80	0.53	0.74	1.11	1.11	1.27	0.27	1.11	0.96
Ta	0.32	0.09	0.30	0.20	0.11	0.06	0.06	0.11	0.04	0.41	0.04	0.02	0.06
La	14.19	14.21	18.31	12.17	10.56	8.91	11.22	11.22	8.91	9.88	3.63	8.91	7.59
Ce	12.32	11.58	28.16	12.91	13.20	10.56	21.12	17.60	15.84	18.38	9.33	14.96	14.08
Pr	1.23	1.51	2.20	1.87	1.57	1.12	1.79	2.02	1.74	2.36	1.01	1.79	1.46
Nd	4.20	4.43	9.00	5.15	4.80	3.60	6.60	6.60	7.20	9.14	3.60	7.20	6.60
Sm	0.91	0.89	1.63	1.43	0.72	0.85	1.48	1.45	1.63	2.10	0.70	1.54	1.18
Eu	0.28	0.30	0.28	0.46	0.24	0.24	0.52	0.45	0.48	0.78	0.21	0.54	0.39
Gd	0.99	0.99	0.99	1.68	0.95	0.87	2.24	1.99	2.22	2.66	0.99	2.24	1.74
Tb	0.14	0.16	0.12	0.31	0.19	0.17	0.39	0.33	0.37	0.54	0.19	0.37	0.28
Dy	0.95	0.95	0.92	2.40	1.11	1.05	2.92	2.38	2.54	4.01	1.01	2.54	1.94
Ho	0.22	0.22	0.22	0.56	0.21	0.22	0.67	0.55	0.49	0.90	0.21	0.49	0.46
Er	0.60	0.66	0.64	1.22	0.60	0.66	1.80	1.40	1.40	1.81	0.60	1.30	1.20
Tm	0.09	0.08	0.11	0.29	0.09	0.10	0.30	0.21	0.21	0.33	0.09	0.20	0.21
Yb	0.70	0.65	0.80	1.51	0.60	0.64	2.00	1.52	1.60	2.98	0.80	1.42	1.32
Lu	0.12	0.12	0.14	0.21	0.11	0.11	0.31	0.27	0.27	0.43	0.12	0.25	0.21
∑REE	36.94	36.75	63.52	42.17	34.95	29.10	53.36	47.99	44.90	56.30	22.49	43.75	38.66
Eu/Eu*	0.90	0.98	0.67	0.91	0.89	0.85	0.87	0.81	0.77	1.01	0.77	0.89	0.83
$(La/Sm)_N$	10.07	10.31	7.25	5.49	9.47	6.77	4.89	5.00	3.53	3.04	3.35	3.74	4.15
$(Gd/Yb)_N$	1.17	1.26	1.02	0.92	1.31	1.12	0.93	1.08	1.15	0.74	1.02	1.30	1.09
$(La/Yb)_N$	14.54	15.68	16.42	5.78	12.62	9.99	4.02	5.29	3.99	2.38	3.25	4.50	4.12

and $^{36}Ar = 2 \times 10^{-13}$ cm^3 STP. The Ar data was corrected for blanks, mass spectrometer discrimination and nuclear-induced interferences ($^{36/37}Ca = 0.000255$; $^{39/37}Ca = 0.00076$; $^{40/39}K = 0.0085$).

Ar–Ar analyses measured on three dykes, i.e. porphyritic dolerite dyke (KD29, trend N80°E), gabbroic dyke (KD41, trend N60°E) and dolerite dyke (KD16, orientation N50°E) indicate two distinct periods of magmatic activity separated by at least 200 Ma. Isotopic ratios and age data of the dykes presented in Table 2 clearly indicate the best estimation of intrusion age (mean ages) and subsequent thermal histories recorded by minerals and matrix. The first group of the two phases magmatic emplacement yields a mean age of 2219 ± 111 Ma and 2203 ± 168 Ma for two different samples and the second group gives a mean age of 2397 ± 74 Ma (range from

Table 2. Argon isotope and age data for Karimnagar mafic dyke samples

Sample	$^{36}Ar/^{39}Ar$	$^{37}Ar/^{39}Ar$	$^{38}Ar/^{39}Ar$	$^{40}Ar/^{39}Ar$	^{39}Ar	$^{40}Ar/^{39}Ar^*$	Age (Ma)	$\pm(2\sigma)$
KD16	7.487	284.52	n.d.	657.2	0.01	n.d.	0	2180
KD16	1.848	188.38	0.300	563.9	0.01	17.85	309	11697
KD16	0.007	1.29	0.015	139.6	3.82	137.44	1609	26
KD16	0.019	1.86	0.017	159.7	2.86	154.19	1734	33
KD16	0.241	43.59	0.047	236.9	0.17	165.55	1814	312
KD16	0.097	4.77	0.036	194.4	0.34	165.80	1816	134
KD16	0.425	77.69	n.d.	310.8	0.04	185.07	1944	1281
KD16	0.015	10.01	0.023	210.0	0.73	205.67	2072	79
KD16	0.037	6.70	0.051	240.0	0.24	229.12	2207	197
KD16	0.023	4.21	0.015	236.5	0.53	229.81	2211	120
KD16	0.020	14.40	0.023	268.8	0.52	262.90	2386	96
KD16	0.565	107.75	0.109	475.3	0.07	308.24	2601	612
KD16	n.d.	n.d.	n.d.	–836.9	0.00	431.42	3081	6325
Mean							2219	111
KD41	0.505	93.45	0.134	209.4	0.05	60.34	883	1373
KD41	0.286	49.77	0.018	147.2	0.10	62.74	911	760
KD41	0.014	1.50	0.014	89.5	1.69	85.30	1151	43
KD41	0.011	0.90	0.016	91.1	2.66	87.96	1178	26
KD41	0.110	22.76	0.148	162.3	0.10	129.86	1549	517
KD41	0.014	5.85	0.004	147.2	0.50	143.11	1652	77
KD41	0.059	9.76	0.023	171.1	0.22	153.68	1730	151
KD41	n.d.	0.77	0.018	156.8	2.06	157.27	1756	35
KD41	n.d.	0.36	0.008	155.4	2.72	158.93	1768	19
KD41	0.073	8.48	0.005	182.1	0.38	160.39	1778	109
KD41	0.017	0.73	0.003	173.5	2.16	168.51	1834	38
KD41	0.011	0.22	0.015	174.4	4.35	171.06	1852	15
KD41	0.083	11.99	0.025	203.9	0.21	179.43	1907	231
KD41	0.036	11.43	0.076	194.4	0.24	181.85	1923	111
KD41	0.010	0.68	0.008	184.8	2.27	182.02	1924	29
KD41	0.007	0.17	0.013	188.5	4.89	186.41	1953	17
KD41	0.080	5.80	0.027	210.5	0.56	186.93	1956	86
KD41	0.000	1.83	0.016	187.1	1.42	186.98	1956	43
KD41	0.184	6.83	n.d.	246.3	0.23	191.92	1988	144
KD41	0.034	3.60	0.021	217.8	0.94	207.78	2085	58
KD41	0.016	1.68	0.014	223.1	1.44	218.19	2145	37
KD41	0.042	3.45	0.030	276.1	0.66	263.58	2389	56
KD41	0.040	3.90	0.018	279.7	0.59	267.79	2410	61
Mean							2203	168
KD29 A1 white milky field 2	0.021	1.61	0.015	50.2	3.16	44.04	684	11
KD29 A1 white field 2	0.023	3.27	0.014	63.9	2.50	57.18	846	14
KD29 A1 grey field 1	0.061	0.90	0.023	78.6	4.15	60.48	885	11
KD29 A1 white cloudy field 3	0.012	2.01	0.012	80.6	2.55	76.99	1067	13
KD29 A1 mafic 1	0.049	30.98	n.d.	149.0	0.22	134.46	1585	104
KD29 A1 orange yellow field 3	n.d.	32.27	0.007	217.7	0.24	220.13	2157	78
KD29 A1 orange yellow field 4	0.017	17.61	0.042	227.4	0.34	222.24	2169	55
KD29 A1 orange yellow field 5	0.017	14.09	0.017	245.3	0.36	240.23	2268	50
KD29 A1 orange yellow field 2	0.022	15.44	0.000	279.2	0.49	272.70	2434	34
KD29 A1 orange yellow field 1	0.031	17.43	n.d.	283.1	0.48	274.05	2441	32
KD29 A1 orange yellow field 6	0.022	8.46	0.019	280.9	0.31	274.42	2443	64
Mean							2397	74

2268 ± 50 Ma to 2443 ± 64 Ma, Table 2) for their emplacement periods. Younger thermal events around 1585, 1050 and 800 Ma are recorded by mineral and matrix. The younger thermal events recorded at 1585 Ma may be related to mafic mineral resetting, 1050 Ma may be related to granulite metamorphic event and younger event 800 Ma may be resetting of milky white and grey feldspars in the rock. To confirm the results obtained, an integrated approach in terms of field relationships, petrography, geochemical and palaeomagnetic studies clearly supports two phases of dyke activity in the region. The present mafic dyke emplacement coincides with the

ages reported (2.42 ± 0.08 Ga and 2.47 ± 0.03 Ga) by monazites and uranitites from Karimnagar belt[9]. Apart from the magmatic emplacements within the dykes, there are younger thermal events recorded by different minerals like milky white feldspars (684 ± 11 Ma), white feldspar (846 ± 14 Ma) and grey feldspar (855 ± 11 Ma). Metamorphic events represented by clouded feldspar (1067 ± 13 Ma) and mafic minerals (1585 ± 104 Ma) suggest that granulite metamorphism which occurred at 1600 Ma is similar to Eastern Ghats metamorphism or collision related to upliftment/tectonics in the area. These mineral reset ages clearly demonstrate that the area has been subjected to deformation subsequent to the emplacements.

Palaeomagnetism

In the palaeomagnetic studies of 264 cylindrical specimens from 53 samples representing 15 sites, the natural remnant magnetization (NRM) directions of dykes are highly scattered, as is generally the case with several dolerite dykes. However, there is good grouping of specimen vectors in each sample. Characteristic remnant magnetic (ChRM) vectors in these dykes have been investigated by the alternating magnetic field (AF) demagnetization method (Figure 5). Specimens from sites 10 and 13 with east southeast and downward declination with upward and downward pointing inclinations respectively, mostly retain their NRM vectors throughout the magnetization treatment. With the help of pilot demagnetization behaviour of these specimens shown in Figure 6 (ref. 13), peak alternating fields for each site were selected and all the specimens from them were AF demagnetized to recover their characteristic component. Specimen and sample vectors were averaged to obtain sample and site mean vectors by using Fisher statistical methods[14]. The relevant palaeomagnetic parameters for the Karimnagar dyke swarm are listed in Table 3 and the site mean ChRM vectors shown in Figure 7. The palaeomagnetic results of Karimnagar dykes suggest that three ChRM directions of magnetization are evident: one in northeastern quadrant with shallow negative inclination from 12 sites with a mean direction of D_m = 52.5, I_m = –24.5, a second ChRM vector in the east–southeastern quadrant with a mean direction of D_m = 126.2, I_m = –54.7 at site 10 and a third ChRM vector with a mean direction of D_m = 186.6,

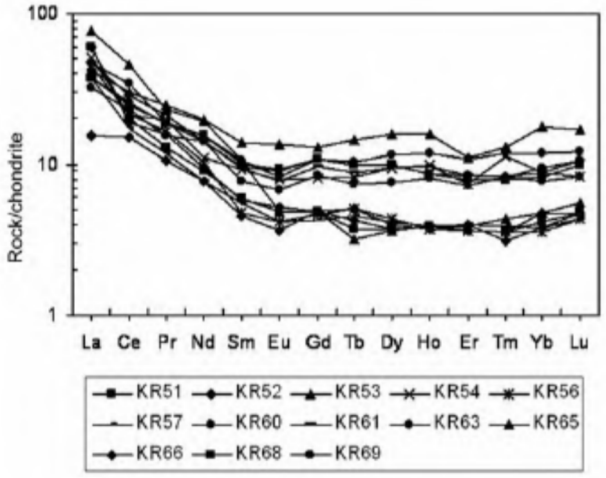

Figure 3. Chondrite normalized rare earth element patterns of Karimnagar dykes.

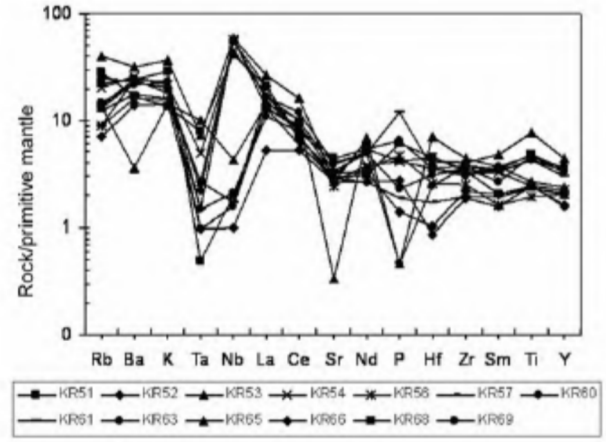

Figure 4. Primitive mantle normalized multielemental spidergram showing nature of two different types of patterns.

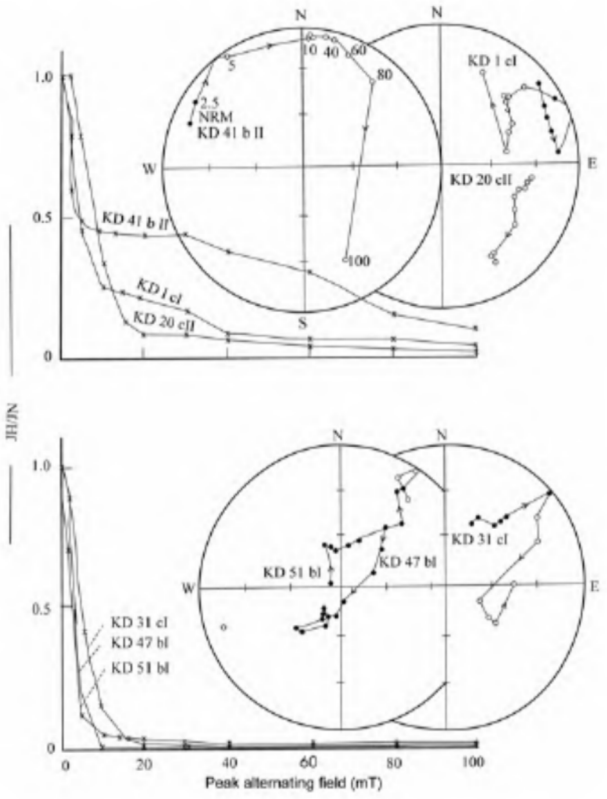

Figure 5. Response of Karimnagar dykes to AF demagnetization. Normalized intensity decay and vector migration for few typical specimens. Open (closed) circles denote upward (downward) inclinations. AF fields are in mT.

Table 3. Remnant magnetic data for the Karimnagar dyke swarm

	Remnant magnetic vector				VGP		
Strike	$N(n)$	D_m	I_m	K	α_{95}	λ_p	L_p
N50°E	6(1)	42.3	–19.1	38.72	10.06	39.8°N	199.1°E
N45°E	3 –	55.8	–20.1	24.72	16.26	28.0°N	191.6°E
N05°E	5 (2)	50.6	–17.9	240.96	5.21	33.1°N	193.2°E
N50°E	3 –	61.8	–44.5	4.41	8.51	15.4°N	203.1°E
N55°E	3 –	70.8	–21.4	3.08	46.07	14.3°N	185.8°E
N50°E	2 –	65.6	–17.7	3.05	56.67	19.8°N	186.2°E
N50°E	3(1)	32.0	–21.0	14.51	25.98	47.0°N	09.3°E
N80°E	2(1)	37.9	–17.8	6.53	31.64	43.6°N	202.3°E
N80°E	3(1)	86.2	–34.9	15.87	24.85	2.6°S	188.5°E
N50°E	2 –	126.2	–54.7	27.78	18.78	39.8°N	160.1°E
N40°E	3 (1)	3.5	–37.2	13.04	27.42	24.5°N	203.5°E
N63°E	10 (1)	43.9	+19.5	11.67	16.68	46.7°N	174.1°E
		43.9	–9.2	10.19	25.32	40.9°N	193.2°E
N60°E	4 (1)	186.6	+49.4	16.78	19.73	40.7°N	251.8°E
N55°E	5 (1)	37.1	–24.9	14.01	18.70	41.6°N	207.3°E
Mean (12 sites)		52.5	–24.5	21.81	8.65	31.9°N	197.1°E

N = No. of samples; K = Precision parameter; n = No. of samples excluded; α_{95} = Radius of 95% confidence circle; D_m = Mean declination; λ_p = Latitude of VGP; I_m = Mean inclination; L_p = Longitude of VGP.

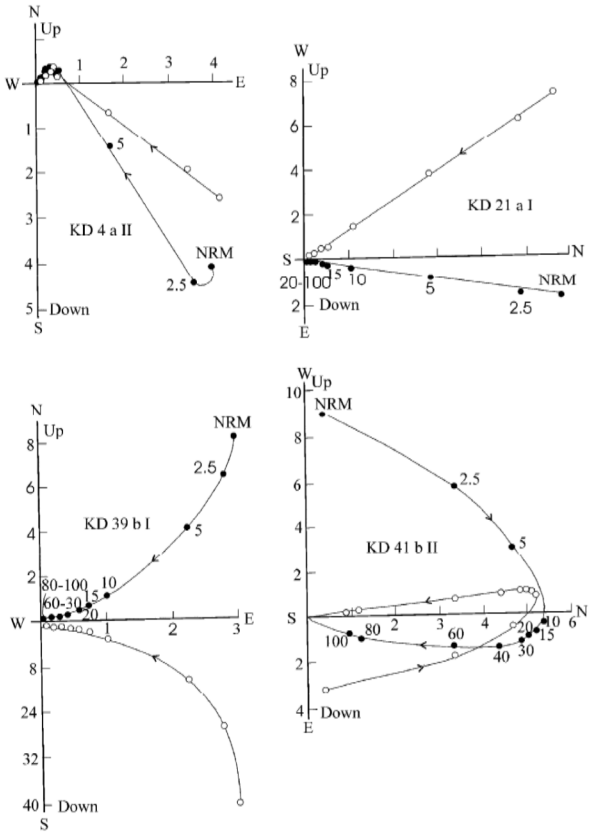

Figure 6. Zijderveld plot of AF demagnetization characteristics of dykes. Closed (open) circles denote end point of remnant vector on horizontal (vertical) planes. Intensities are of mA/m order.

I_m = +49.4 from site 13. Thus, three different ChRM vectors observed along this dyke swarm may represent multiple igneous activities as recorded by earlier workers[15].

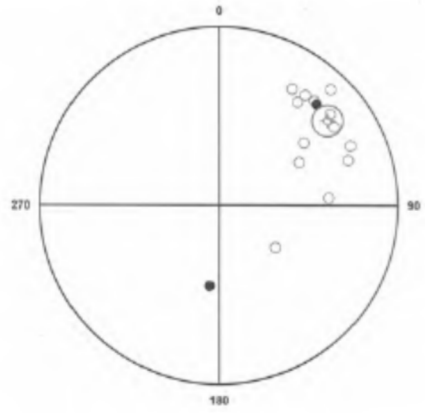

Figure 7. Stereographic projection showing site mean remnant magnetic vectors for Karimnagar dykes. Open (closed) circles denote upward (downward) inclinations. Mean (12 sites) is shown with horns.

Discussion

Mafic dykes are important features of the Proterozoic period and act as potential time markers in parts of stabilized Archaean cratons. During the Proterozoic time, growth of continents took place by the addition of mantle derived juvenile material to pre-existing continental blocks. This accretion took place largely within three tectonic environments within the supercontinents or large continental blocks that underwent rifting and breakup giving rise to continental flood basalts and mafic dyke swarms[16], and the examples are giant mafic dyke swarms worldwide at 2.4–2.0 Ga[17,18] including the Karimnagar dyke swarms[19], mafic dykes of southeast Mysore[6,20–22], Cuddapah dyke/dyke swarms[8] and other Indian dyke swarms. In the Karimnagar area, fault/lineament is controlled in NE–ENE and NW–WNW directions, parallel to

the dyke swarms and Godavari–Pranhita rift axis respectively. None of the dykes is seen cutting the Gondwana Formation of Carboniferous–Jurassic age. The age data from Karimnagar belt and Bhopalpatnam granulite belts are considered to be a single terrain and the mid-Archaean to early Proterozoic signature recognized in KGB is totally missing[9]. The possibility of extension of these mafic dykes under the sedimentary cover through the BGB may be checked and if present, then the linking of these two terrains of KGB and BGB to Godavari Granulite Belt will be interesting. The petrographic and geochemical results suggest at least two distinct groups of dykes among the Karimnagar dyke swarm namely quartz normative and olivine normative tholeiites. The higher Cr and Ni and more calcic plagioclase in quartz normative types suggest that they belong to early intrusive phase (2400 Ma) than the olivine normative type (2200 Ma). Exact demarcation cannot be drawn in the field between the two types of dolerite and gabbro dykes present in granulite and non-granulite terrain, but they show distinct petrographic and geochemical signatures between them. The orientation of the dyke swarm and its orthogonality to the Godavari–Pranhita rift suggests that the dykes were emplaced along the older Precambrian crustal fractures which may be related to Palaeoproterozoic breakup of the supercontinent. Recently a large number of 2.5–2 Ga magmatic, detrital and xenocratic ages have been reported from all the cratonic blocks of Indian Shield, Zimbabwe, Kaapvaal and Pilbara cratons[21]. A common remnant magnetic vector of $D_m = 52.5$, $I_m = -24.5$ ($K = 21.81$, $\alpha_{95} = 8.65$ and $N = 12$) was achieved along with two other minor vectors in the ESE and S quadrants with steep upward and downward inclinations respectively. Thus this integrated geochronological, petrological, geochemical and palaeomagnetic studies clearly support a minimum of two intrusive phases of magmatism along with two more minor phases of dyke activity in the Karimnagar region dykes. Mafic dyke swarms represent short-lived magmatic events that carry important and chemical constraints for the evolution of the lithospheric mantle.

1. Windley, B. F., *The Evolving Continents*, Wiley, Chichester, 1995, 3rd edn.
2. Heaman, L. M., Global mafic magmatism at 2.45 Ga: remnants of an ancient large igneous province?. *Geology*, 1997, **25**, 299–302.
3. Halls, H. C., Kumar, A., Srinivasan, R. and Hamilton, M. A., Palaeomagnetism and U–Pb geochronology of easterly trending dykes in the Dharwar craton, India: feldspar clouding, radiating dyke swarms and position of India at 2.37 Ga. *Precambr. Res.*, 2007, **155**, 47–68.
4. Ernest, R. E. and Srivastava, R., Proterozoic record of large igneous provinces (LIPs) of Indian shield: evidence from mafic dyke swarms and related magmatic units. 6th International Dyke Conference, Varanasi, 4–7 February 2010, p. 149.
5. Murthy, N. G. K., Proterozoic mafic dykes in southern Peninsular India: a review. Dyke swarms of India. *Mem. Geol. Soc. India*, 1995, **33**, 81–98.
6. Devaraju, T. C., Viljoen, R. P., Sawkar, R. H. and Sudhakar, T. L., Mafic and ultramafic magmatism and associated mineralization in the Dharwar craton, southern India. *J. Geol. Soc. India*, 2009, **73**, 73–100.
7. Mallikharjuna Rao, J., Bhattacharji, S., Rao, M. N. and Hermes, O. D., ^{40}Ar–^{39}Ar ages and geochemical characteristics of dolerite dykes around the Proterozoic Cuddapah Basin, South India. *Mem. Geol. Soc. India*, 1995, **33**, 307–328.
8. French, J. E., Heaman, L. M., Chacho, T. and Srivastava, R. K., 1891–1883 Ma southern Bastar–Cuddapah mafic igneous events, India: a newly recognized large igneous province. *Precambr. Res.*, 2008, **160**, 308–322.
9. Santosh, M., Yokoyama, K. and Acharyya, S. K., Geochronology and tectonic evolution of Karimnagar and Bhopalapatnam Granulite Belts, Central India. *Gondwana Res.*, 2004, **7**, 501–518.
10. Mallikharjuna Rao, J., Rao, G. V. S. P. and Patil, S. K., Geochemical and palaeomagnetic studies on the Middle Proterozoic Karimnagar mafic dyke swarm, India. In *Mafic Dykes and Emplacement Mechanisms* (eds Parker, A. J., Rickwood, P. C. and Tucker, D. H.), Balkema, Rotterdam, 1990, pp. 373–382.
11. Sharma, I. N. and Prakash, D., Reaction textures and P–T conditions of Opx-Crd gneisses from Karimnagar, Andhra Pradesh, India. *Mineral. Petrol.*, 2007, **90**, 175–197.
12. Rajesham, T., Bhaskar Rao, Y. J. and Murti, K. S., The Karimnagar granulite terrane – a new sapphirine bearing granulite province, South India. *J. Geol. Soc. India*, 1993, **41**, 51–59.
13. Zijderveld, J. D. A., A.C. demagnetization of rocks: analysis of results. In *Methods in Palaeomagnetism* (eds Collinson, D. W., Creer, K. M. and Runcorn, S. K.), Elsevier, New York, 1967, pp. 254–286.
14. Fisher, R. A., Dispersion on a sphere. *Proc. R. Soc. London Series A*, 1953, **217**, 295–305.
15. Subba Rao, Y. V. and Radhakrishna Murthy, I. V., Palaeomagnetism and age of dolerite dykes in Karimnagar District, Andhra Pradesh, India. *Geophys. J. R. Astron. Soc.*, 2007, **82**, 331–337.
16. Windley, B. F., Continental growth in the Proterozoic: a global perspective. Proterozoic East Gondwana: supercontinent assembly and breakup (eds Yoshida, M., Windley, B. F. and Dasgupta, S.), Geol. Soc. Spl. Publ., 2003, p. 206.
17. Ernst, R. E. and Buchanan, K. L. (eds), Large mafic magmatic events through time and links to mantle plume heads. In *Mantle Plumes: Their Identification through Time*, Geol. Soc. Am. Spl. Pap., 2001, vol. 352, pp. 483–575.
18. Vogel, D. C., Vuollo, J. I., Alapieti, T. T. and James, R. S., Tectonic, stratigraphic and geochemical comparison between ca 2500–2440 Ma mafic igneous events in the Canadian and Fennoscandian shields. *Precambr. Res.*, 1998, **92**, 89–116.
19. Kumar, A., Halls, H. C. and Hamilton, M. A., Palaeomagnetism and U–Pb geochronology of the Karimnagar dykes, Dharwar Craton, India. 6th International Dyke Conference, Varanasi, 4–7 February 2010, p. 6.
20. Ikramuddin, M. and Steuber, A. M., Rb–Sr ages of Precambrian dolerite and alkaline dykes, southeast Mysore State, India. *Lithos*, 1976, **9**, 235–241.
21. Mondal, M. E. A., Faruq Hussain, M. and Ahmad, T., Mafic dyke swarms of Central Indian Shield: implications for a Pre-Rodinia Supercontinent Assembly. 6th International Dyke Conference, Varanasi, 4–7 February 2010.
22. Srivastava, R. and Gautam, G. C., Precambrian mafic magmatism in the Bastar craton, Central India. *J. Geol. Soc. India*, 2009, **73**, 52–72.
23. LeBas, M. J., LeMaitre, R. W., Streckeisen, A. and Zanettin, B., A chemical classification of volcanic rocks based on the total alkalies–silica diagram. *J. Petrol.*, 1986, **27**, 745–750.
24. Macdonald, G. A. and Katsura, T., Chemical composition of Hawaiian lavas. *J. Petrol.*, 1964, **5**, 82–133.

ACKNOWLEDGEMENTS. J.M.R. and G.V.S.P.R. thank the Director, NGRI, Hyderabad, for his interest in these studies and permission to publish the results. M.W. acknowledges the financial support of NERC grant during the course of research work.

Received 12 August 2009; revised accepted 23 April 2010